

# Assessment of the Strain Distribution in Wood Adhesive Bonds by Contact-free Measurement and Finite Element Analyses

Erik Serrano<sup>1</sup> and Bertil Enquist<sup>2</sup>

1. SP Swedish National Testing and Research Institute, BORÅS, Sweden.

2. School of Technology and Design, Växjö University, Växjö, Sweden

## Abstract

This article reports on an investigation relating to the strain distribution in wood adhesive bonds. Measurements with a 1.3M ARAMIS system are presented and compared with finite element simulations. The results from tests with two different specimen geometries and three different adhesives are reported. The adhesives tested were a phenolic resorcinol (PRF), a one-component polyurethane (PUR) and an epoxy (EPX). The finite element study included the use of a non-linear fracture mechanics model for the adhesive bond line. The measurements performed show that the different adhesives resulted in different strain distributions at a given load, which can be attributed their different mechanical properties in terms of stiffness and ductility (fracture energy). The brittle PRF adhesive showed more localised strains than the more ductile EPX and PUR adhesives did at the same load level. As expected from a theoretical point of view, the two specimen geometries tested showed different strain distributions. Another conclusion drawn is that the measurement technique is very useful in terms of providing detailed data, i.e. at a high level of spatial resolution, for calibration of numerical models.

## Introduction

### Background

Although adhesive technology has been used since historic times for wood-based applications, the state of knowledge concerning the basic mechanical behaviour and requirements is still poor in practice. For example, it is often stated that wood adhesive bonds showing adherend failure are adequately designed, so that no further attention needs to be given to the design of the bond line. It is however well known within the scientific community that not only the bond line and adherend strengths, but also the ductility (or brittleness) of the bond line, are important parameters for the load-bearing capacity of an adhesive joint. By ductility is here meant the joint's capability to produce a uniform stress distribution for a given load. This capability, which obviously is of great importance for producing joints with a high load bearing capacity, is in turn dependent on the joint geometry, the stiffness and strengths of the materials, the plastic behaviour of the joint and its fracture energy. Thus, knowing the stress, or the strain, distribution in a joint is crucial for determining the ductility of the bond line.

Typically, tests on wood adhesive bonds are focused on determining the load-deformation response of a standardised specimen, this being done by sampling the load applied by the testing machine, and the movement of the testing machine's cross-head. Small clip-gauges or LVDTs can be attached to selected parts of the specimen in order to obtain more detailed information, or one could alternatively glue strain gauges into the bond line. Such measurements are, however, restricted in terms of spatial resolution, and it is therefore difficult to obtain any detailed information on the strain distribution along the joint.

## Previous work

DIC-techniques have been used for wood-based materials, although references are scarce. In relation to wood adhesive bonds, only in-plane measurements have been reported (Zink 1992; Zink et al. 1995). In very recent work the strain distribution in wood adhesive joints was studied, by use of electronic speckle interferometry (ESPI), (Müller et al. 2005; Gindl et al. 2005). Such techniques are, however more complicated to use if large strains, beyond the elastic limit, are to be monitored.

## Aim

The work reported herein was performed in order to investigate the possibility of using DIC for measuring the strain distribution in wood adhesive bond lines. Main focus has been on determining the strain distribution obtained for different adhesives. As explained above, the strain distribution is dependent on the mechanical properties of the adhesive. Also the influence of using a different test specimen for one of the adhesives was investigated.

Some numerical finite element results are also reported. These were performed for comparison with the experimental results. The aim was not to obtain accurate fits to the experimental results, but to determine whether these test results, and especially the strain distributions obtained from the ARAMIS system were plausible.

For a more detailed account of the mechanical behaviour of the test specimens, including the type of specimens used here, reference is made to (Serrano 2004). In a recent publication this investigation is presented in more detail (Serrano and Enquist 2005).

## Materials and methods

### Experimental

All the specimens were manufactured from Beech (*Fagus sylvatica L.*). The adhesives used in the investigation were a phenolic resorcinol (PRF), a 2-component polyurethane (PUR) and an epoxy (EPX). The geometries of the test specimens, which are according to the European standard EN 302-1 and the US standard ASTM D905, are shown in Figure 1. Note that especially the EN 302-1 specimen is small, the overlap length which is tested is only 10 mm.

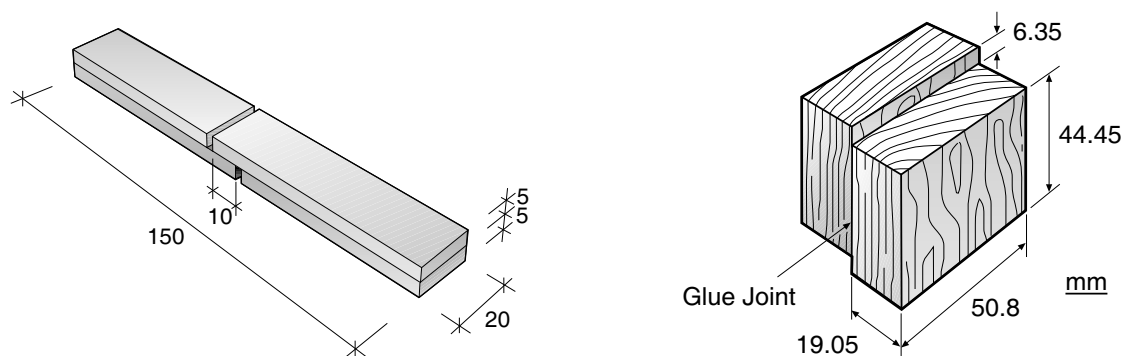


Figure 1. Geometry of the test specimens. Left: EN302-1. Right: ASTM-D905.

Since the test specimens are different, the nominal shear strength obtained from the respective tests is expected to differ, the smaller overlap of the EN 302-1 specimen should give a more uniform shear stress distribution. Figure 2 shows the test set-up for the two specimens.

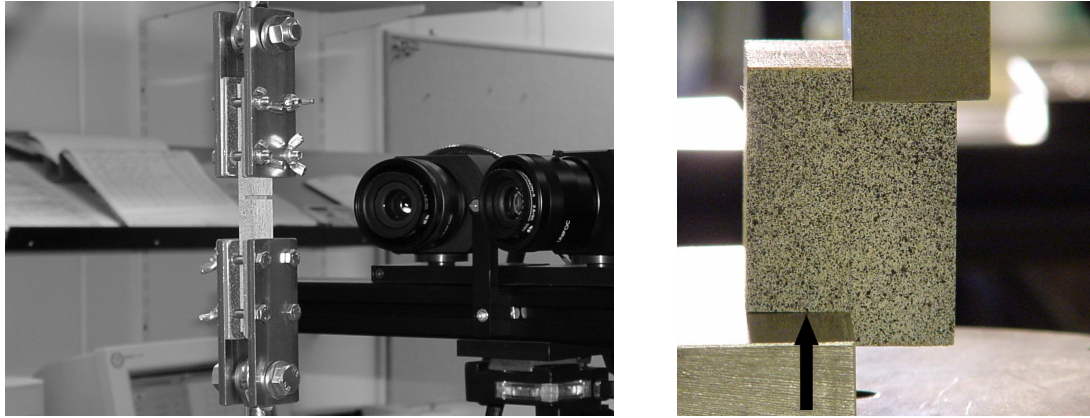


Figure 2. Left: EN 302-1 specimen with cameras. Right: ASTM specimen with speckle pattern applied. The arrow indicates the load direction of the cross head.

### Contact free measurement system

A 1.3M ARAMIS system was used. The speckle pattern was achieved by applying white and black spray paint on the specimens prior to testing.

Frame grabbing was achieved by adjusting the time interval so as to obtain 50-100 pairs of pictures during each test. The load and displacement signals from the testing machine were also sampled when taking each pair of pictures.

The settings used for the ARAMIS system gave a spatial resolution of approximately 0.2 mm for the EN 302 specimen. A slightly different set-up was used for the ASTM specimen, resulting in a spatial resolution of approximately 0.3 mm.

### Numerical methods

#### Geometry, loading conditions and material modelling

Only FE-results relating to the EN302 specimen are presented, this being chosen for its relative simplicity in terms of modelling. The ASTM specimen is more complex to model, mainly due to the fact that its behaviour is strongly affected by local crushing in a narrow zone close to the bond line.

Figure 3 shows the 2D plane strain model of the EN302, consisting of approximately 3600 elements and 7450 nodes, resulting in 14900 degrees of freedom.

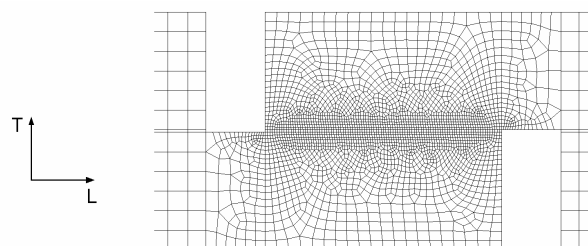


Figure 3. Close-up of the FE-mesh at the bond line of the EN 302-1 specimen.

The elastic constants used for the wood material were  $E_L=11600$ ,  $E_R=2200$ ,  $E_T=1140$ ,  $G_{LR}=1610$ ,  $G_{LT}=1060$  and  $G_{RT}=640$  MPa for the moduli of elasticity and the shear moduli, and  $\nu_{LR}=0.45$ ,  $\nu_{LT}=0.52$  and  $\nu_{RT}=0.71$  for Poisson's ratios. The indices L, R and T denote the

longitudinal, radial and tangential direction, respectively, of the assumed orthotropic material as indicated in Figure 3.

The bond line thickness was set to 0.1 mm in the FE-model. The thickness was also measured in a microscope and was found to vary between 0.1-0.2 mm. A nonlinear fracture mechanics model was used to simulate the behaviour of the bond line. The model employed is described in detail in (Serrano and Gustafsson 1999; Serrano 2004). It takes into account the strain softening behaviour of the bond line in both shearing mode (mode II) and tensile opening mode (mode I). The model also takes into account the coupling effect meaning that the local strength and the fracture energy both depend on the degree of mixed mode.

Two sets of input data, one set to model a brittle and one to model a ductile adhesive, were employed. The input data are estimates based on previous experimental investigations (Serrano 2004) and are not fitted to the actual adhesives used here. The parameters of the bond line model are the uniaxial softening behaviours in modes I (opening mode) and II (shear mode). Piecewise linear stress versus deformation curves, see Table 1 and Figure 4, are used as input to the model. In this particular case the fracture energies are approximately the same for the two adhesives, and the ductility is defined not by the fracture energy, but rather in terms of the slope of the descending part of the stress-versus-deformation curve, as described in (Serrano and Gustafsson 1999; Serrano 2004).

Table 1. Summary of the bond line properties of two types of adhesives.

Adhesive	Mode I		Mode II	
	Strength (MPa)	Fracture energy (J/m <sup>2</sup> )	Strength (MPa)	Fracture energy (J/m <sup>2</sup> )
Brittle	6	550	18	1250
Ductile	6	550	12	1230

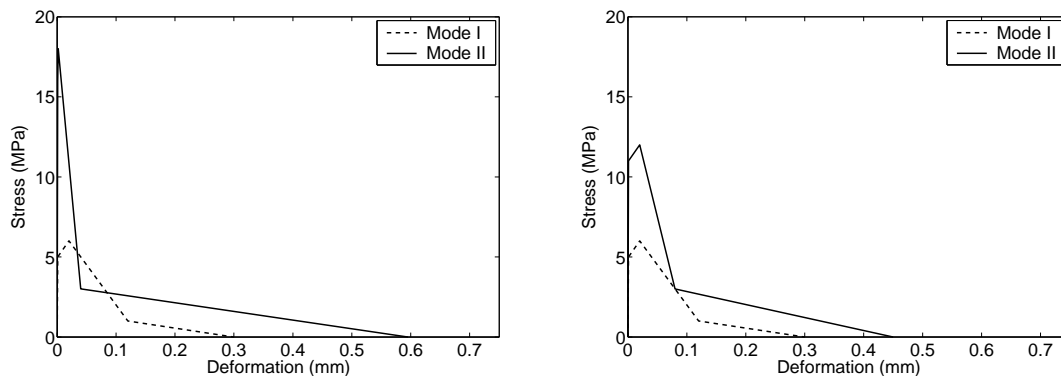


Figure 4. Uniaxial behaviour of the bond line model for a brittle adhesive (left) and a ductile adhesive (right).

## Results

The EN302 specimens at 10 MPa nominal shear stress were used for investigating differences in strain distributions.

In Figure 5, the shear strain is plotted for a path along the bond line glued with the three adhesives, at a nominal shear stress of 10 MPa. At this stage, the PUR is the more ductile one, the EPX and the PRF adhesives showing smaller shear strain angles.

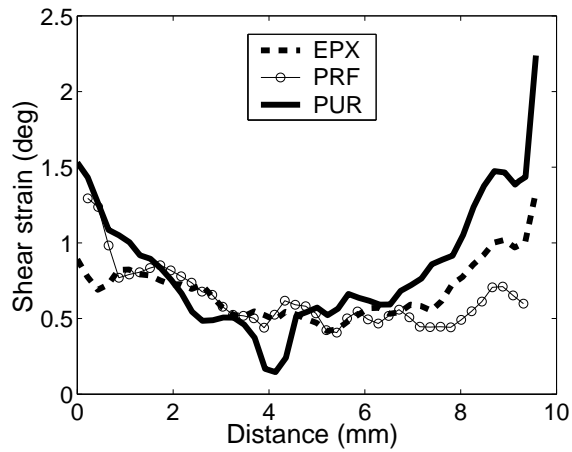


Figure 5. Shear angle distribution in the bond line of the EN302 specimen at 10 MPa shear stress.

In the upper part of Figure 6, the shear strain distribution, at 10 MPa nominal shear stress, is shown. The results from the FE-analyses are shown in the lower part of Figure 6. Note that the same scale is used for the test results and for the FE-results.

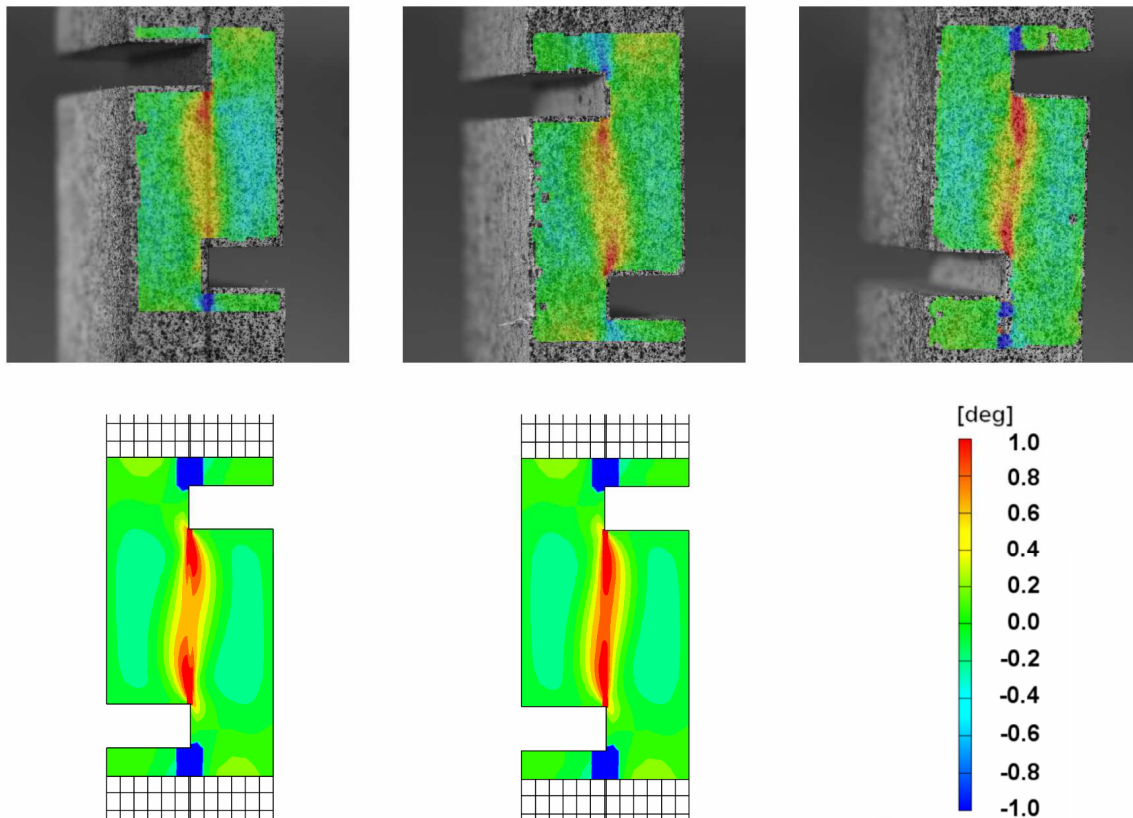


Figure 6. Strain distributions at nominal shear stress of 10 MPa. Top row: Shear angles from tests of the PRF, EPX and PUR adhesives (from left to right). Bottom row: Shear angles from FE-analyses of brittle and ductile bond line behaviour (from left to right). The same scale is used for all plots.

The results from the test with the ASTM-specimen are shown in Figure 7, for this specimen at a nominal average shear stress of 6 MPa. As can be seen, the lower part of the bond line has begun to fail, as shown both by the large area that is highly strained and by the strain values found at distances of more than 20 mm. As mentioned, the spatial resolution in the measurements of the ASTM specimen was about 0.3 mm. This results in a smoother shear strain plot compared to the one shown in Figure 5, since the lower resolution implies that every calculated point represents the average of a larger area.

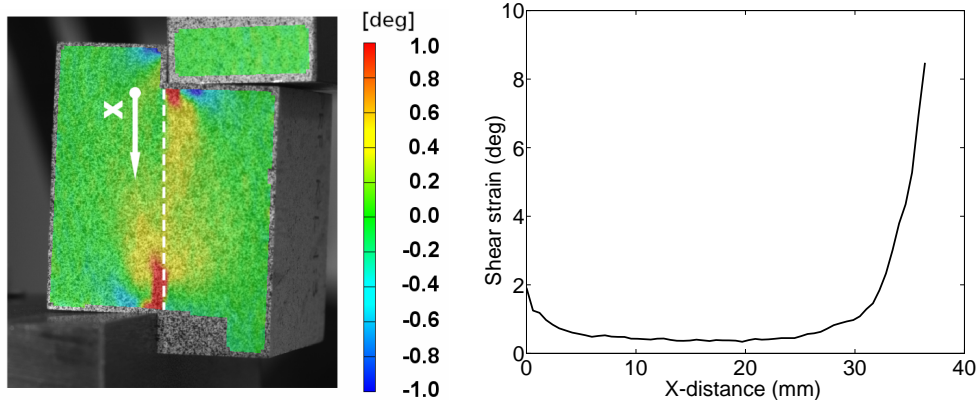


Figure 7. Bond line shear angle in the ASTM specimen at 6 MPa shear stress as determined by tests.

## Discussion and conclusions

The strain distributions obtained from the ARAMIS measurements and from the FE-analyses are similar in terms of at least two major features; the size of the zone containing large shear strain angles (greater than 1 degree) and the S-shape of the highly strained zones, see Figure 6. Note also that the more brittle adhesive (PRF) shows more localised strains than the more ductile one (PUR) does, which is fully in line with the discussion on ductility in the introduction. Thus, it is possible to distinguish from each other, on the basis of the ARAMIS measurements, adhesives that are markedly different from each other in terms of flexibility and ductility.

The results obtained for the ASTM specimen as shown in Figure 7, indicate that the strain distribution is different from that of the EN302 specimen, Figure 5. Although the nominal shear stress is higher for the EN302 specimen results, the strain distribution is more localised in the ASTM specimen in Figure 7. The measurement technique employed is thus capable of distinguishing the different mechanical behaviours of these two standardised test methods.

Using techniques such as the one described here does not exclude the need for conventional measurement techniques, nor does it replace traditional finite element analyses. Instead, such techniques should be considered as a complement to the traditional ones, giving strain distributions with a high degree of spatial resolution in situations in which traditional strain gauges or transducers cannot be used. There is also a large potential for use of the measurement technique in the design of experimental set-ups and for the verification and calibration of numerical simulations. In such cases it is important to use a concurrent engineering approach that involves an active and iterative collaboration between expertise within the experimental and theoretical fields. Another area of application in which the contact-free measurement technique could prove useful is in situations in which the test object would be severely affected by any other means of measuring deformations, which is often the case in testing thin films or paper. Finally, for testing at high temperatures or high humidities,

use of a contact-free technique could well be the only approach to measuring deformations available.

## **Acknowledgements**

This work was made possible through to the financial support of the Swedish Research Council for Environment, Agricultural Sciences and Spatial Planning (FORMAS). The work was carried out at SP – Swedish National Testing and Research Institute and at the Division of Structural Mechanics at Lund University. Special thanks is directed to Mr. Thord Lundgren from Structural Mechanics for his invaluable help with the test procedures and also to GOM GmbH in Germany and Cascade Computing AB in Sweden for use of the measurement equipment.

## **References**

Gindl, W., Sretenovic, A., Vincenti, A. and Müller, M. (2005) Direct measurement of strain distribution along a wood bondline. Part II. Effects of adhesive penetration on strain distribution. *Holzforschung*, Vol. 59, pp.307-310, Walter de Gruyter.

Müller, M., Sretenovic, A., Vincenti, A. and Gindl, W. (2005) Direct measurement of strain distribution along a wood bondline. Part I. Shear strain concentration in a lap joint specimen by means of electronic speckle pattern interferometry. *Holzforschung*, Vol 59, pp. 300-306, Walter de Gruyter.

Serrano, E. and Enquist, B. (2005) Contact free measurement and non-linear finite element analyses of strain distribution along wood adhesive bonds. *Holzforschung*, Vol 59. pp. 641-646, (In press).

Serrano, E. (2004) A Numerical Study of the Shear-Strength-Predicting Capabilities of Test Specimens for Wood-Adhesive Bonds. *International Journal of Adhesion and Adhesives*. 24 (1) pp. 23-35

Serrano, E. and Gustafsson, P. J. (1999) Influence of bondline brittleness and defects on the strength of timber finger-joints. *International Journal of Adhesion and Adhesives*. 19 (1) pp. 9-17.

Zink, A. G. (1992) The influence of overlap length on the stress distribution and strength of a bonded wood double lap joint. PhD thesis. State University of New York, Syracuse, USA.

Zink, A. G., Davidson, R. W., Hanna Robert, B. (1995) Strain measurement in wood using a digital image correlation technique. *Wood and fiber science* 27(4):346-359